surfaces

Spontaneous Grafting of OH-Terminated Molecules on Si–H Surfaces via Si–O–C Covalent Bonding

Essam M. Dief [1], Anton P. Le Brun [2], Simone Ciampi [1] and Nadim Darwish [1,*]

Supplementary materials

1. XPS analysis

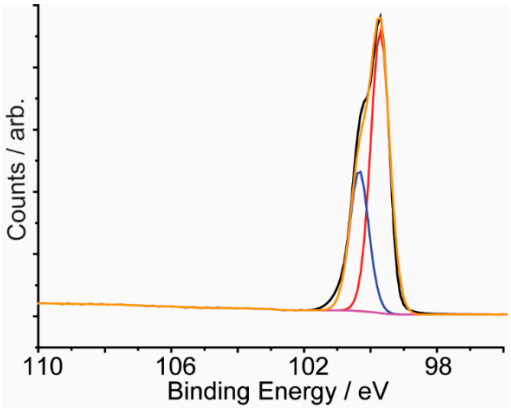

Figure S1. Si 2p high resolution spectrum for a freshly prepared Si–H surface, after the etching step. The absence of emission at ~103 eV demonstrates that the starting Si–H surface is free of oxide.

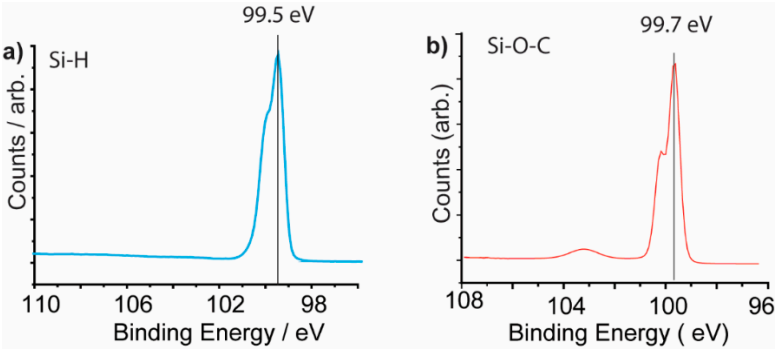

Figure S2. XPS analysis showing high resolution Si 2p signal from a pure Si–H surface (a) and a Si surface functionalized with **1,** showing that surface functionalization shifts the Si peak to slightly higher binding energy. All peak energies were calibrated by applying a rigid shift to bring the C 1s emission to 284.7 eV.

2. X-ray Reflectometry (XRR) analysis

X-ray reflectometry (XRR) was recorded at the solid-air interface with a radiation source (Cu Kα radiation, λ = 1.54 Å) from a Panalytical Ltd X'Pert Pro. A Göbel mirror was used to focus the X-ray beam and a motorized stage was used to optimize the sample position. Bean incidence angles were measured from 0.05° to 5.00° in 0.01° steps (20 seconds per each step). The critical edge within the raw data was normalized to a reflectivity of unity. Data was presented as reflectivity versus momentum transfer (Q). Q is defined as: $Q = (4\pi \sin\theta)/\lambda$, where θ is beam incidence angle and λ is the X-ray beam wavelength. The data was analyzed by REFNX [1] which utilizes an Abele's matrix method and a genetic algorithm to minimize χ^2 values to achieve the best fit to the data. The SAM was

fitted using a single layer model with fitting parameters of thickness, roughness, and scattering length density (SLD), ϱ, defined as: $\varrho = (r_e \sum Z_i) / V_m$, where V_m is the total molecular volume, Z_i is the atomic number of each atom in the species, and r_e is the Bohr electron radius (2.818×10^{-5} Å). The fitting parameters were changed using least-squares regression until the calculated reflectivity from the fitting suitably matched the collected data. The number of molecules per cm² was determined from the fitted values as follows: molecules per $cm^2 = (\tau \varrho_f 10^{16}) / (V_m \varrho_t)$, where τ is the fitted thickness and ϱ_f is the fitted SLD.

Table S1. Fitted thicknesses, surface roughness, and fitted SLD for SAMs formed from **1** and **2** on Si (111)–H as determined from XRR data.

Monolayer	Thickness / Å	Fitted SLD / $\times 10^{-6}$ Å^{-2}	Volume fraction	Molecules per cm²	Fitted Roughness / Å (silicon-monolayer / monolayer-air)
SAM of **1** on Si	7.2	14.09	0.996	3.99×10^{14}	5.1/4.6
SAM of **2** on Si	5.8	13.14	0.951	3.35×10^{14}	3.7/4.4

3. AFM topography imaging

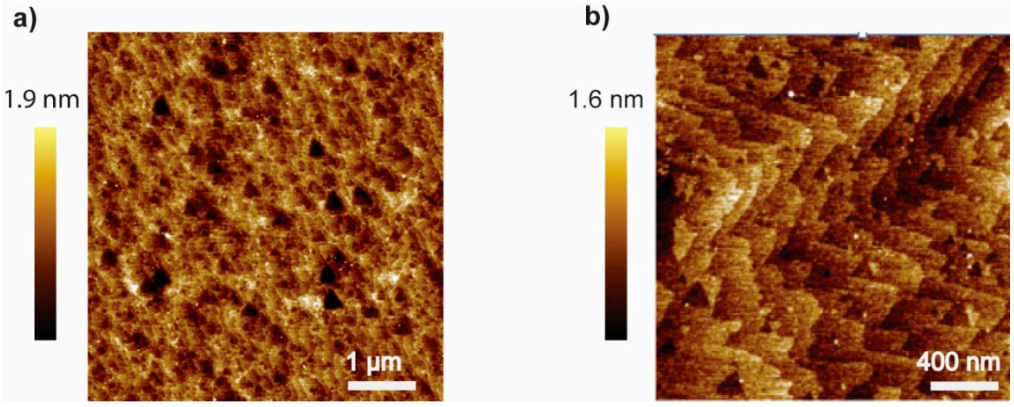

Figure S3. AFM topography images with large scan area (a) and small scan area (b) for Si–H surface without SAMs showing flat Si (111) terraces and smooth edges. The surface roughness analysis showed large flat terraces with smooth atomic edges and peak-to-peak roughness of ~0.21 nm within an individual terrace. This is consistence with monolayers formed with other methods on Si–H surfaces[2,3].

4. Electrochemical characterization

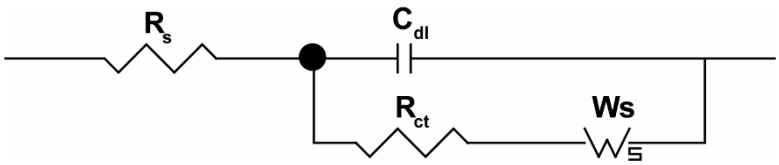

Figure S4. Equivalent circuit for the Nyquist plots of the EIS measured for the SAM of **2** on Si–H and the fresh Si–H surfaces. R_{ct} of ~1187 Ω and ~4571 Ω for the bare Si–H and the functionalized Si surface respectively, is expected on the basis that a monolayer can partially block charge transfer at the interface and therefore increase the charge transfer resistance.

References

1. Nelson, A.R.J. and Prescott, S.W. *refnx:* neutron and X-ray reflectometry analysis in Python. *J Appl Crystallogr*, **2019**, **52**(Pt 1): pp. 193–200.
2. Vogel, Y.B., et al. Reproducible flaws unveil electrostatic aspects of semiconductor electrochemistry. *Nat. commun.*, **2017**, **8**(1): pp. 2066–2066.
3. Dief, E.M., Vogel, Y.B., Peiris, C.R., Le Brun, A.P., Gonçales, V.R., Ciampi, S., Reimers, J.R. and Darwish N. Covalent linkages of molecules and proteins to Si–Hsurfaces formed by disulfide reduction. *Langmuir*, 2020, 36, 49, 14999–15009.